

Electronic Supplementary Information

Improvement of Efficiency and Its Roll-off at High Brightness in White Organic Light-Emitting Diodes by Strategically Managing Triplet Excitons in Emission Layer

Shian Ying,^a Dezhi Yang,^a Xianfeng Qiao,^a Yanfeng Dai,^a Qian Sun,^a Jiangshan Chen,^a Tansir Ahamad,^b Saad M. Alshehri^b and Dongge Ma^{*ab}

^a Center for Aggregation-Induced Emission, Institute of Polymer Optoelectronic Materials and Devices, State Key Laboratory of Luminescent Materials and Devices, South China University of Technology, Guangzhou, 510640, People's Republic of China.

E-mail: msdgm@scut.edu.cn

^b Department of Chemistry, King Saud University, Riyadh, Kingdom of Saudi Arabia

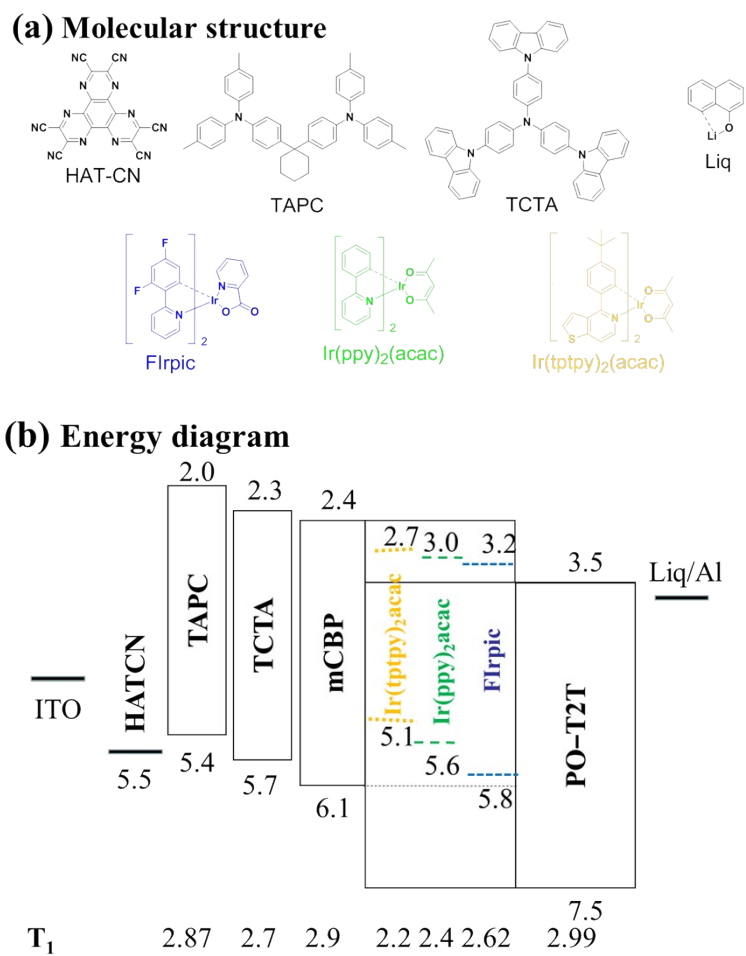


Fig. S1. (a) Chemical structures of the organic materials used in this study. (b) Proposed energy level diagram of the fabricated devices.

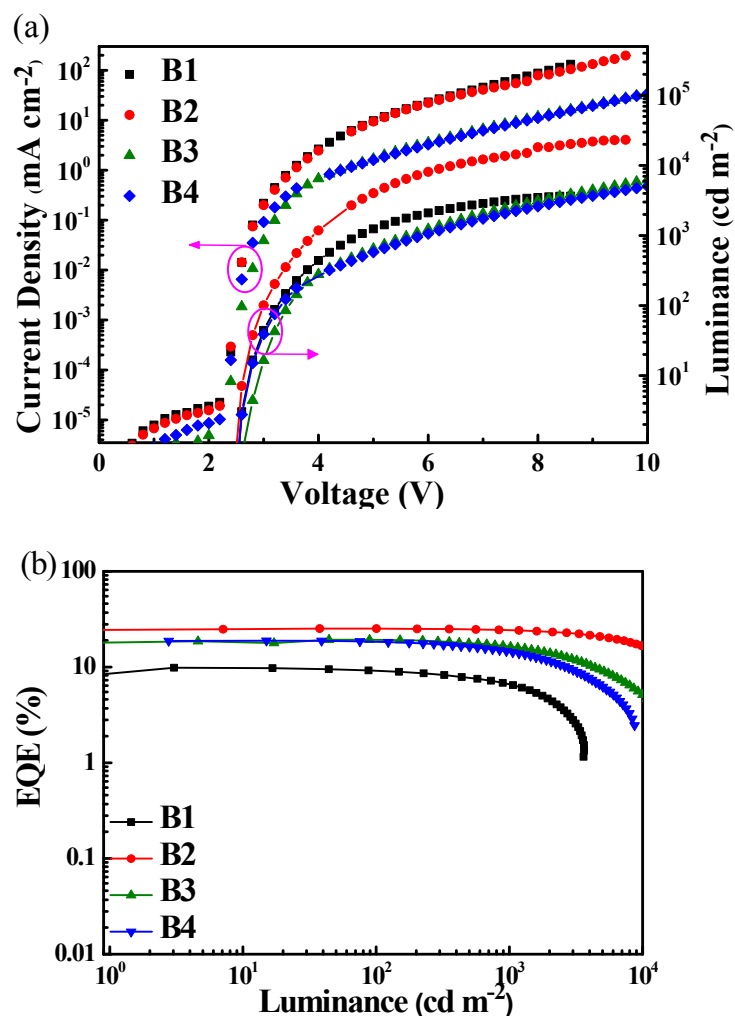


Fig. S2. (a) Current density–luminance–voltage (J–L–V) characteristics and (b) external quantum efficiency versus luminance characteristics of the blue devices. The device structure is ITO / HATCN (15 nm) / TAPC (60 nm) / TCTA (5 nm) / mCBP (5 nm) / EMLs / PO-T2T (45 nm) / Liq (1.5 nm) / Al (150 nm). EML of B1: mCBP:PO-T2T (1:1, 15 nm). EML of B2: mCBP:PO-T2T:FIrpic (1:1:10%, 15 nm). EML of B3: mCBP:FIrpic (1:10%, 15 nm). EML of B4: PO-T2T:FIrpic (1:10%, 15 nm).

Table S1. EL characteristics of the blue OLEDs.

Device	V_{on}^a (V)	L_{max}	PE_{max}	PE^b	LE_{max}	LE^b	EQE_{max}	EQE^b
		($cd\ m^{-2}$)	($lm\ W^{-1}$)	($lm\ W^{-1}$)	($cd\ A^{-1}$)	($cd\ A$)	(%)	(%)
B1	2.5	3639	25.7	8.9	21.3	13.6	9.9	6.5
B2	2.5	19660	59.9	39.0	50.3	48.4	25.2	24.3
B3	2.7	14210	45.9	18.9	42.7	34.9	19.3	16.3
B4	2.6	8883	51.2	16.9	42.8	32.4	18.8	14.2

Abbreviations: V_{on} : turn-on voltage. L_{max} , PE_{max} , LE_{max} and EQE_{max} : maximum luminance and efficiencies.

^a Recorded at $1\ cd\ m^{-2}$. ^b Recorded at $1000\ cd\ m^{-2}$.

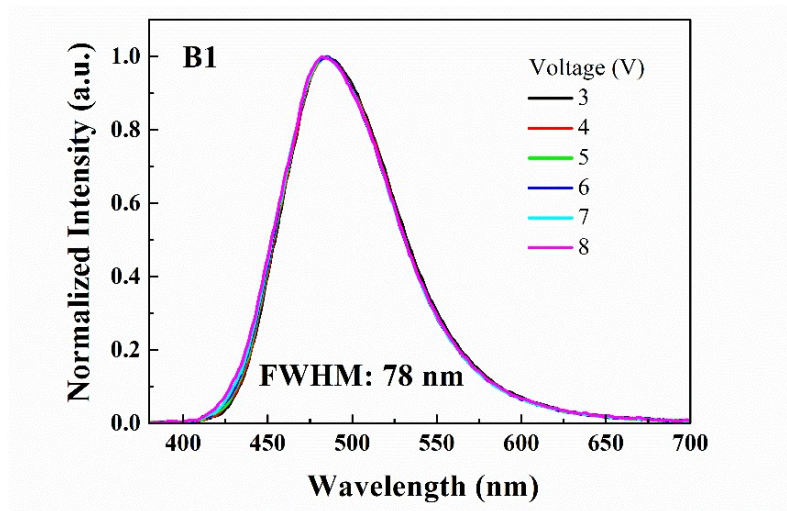


Fig. S3. Normalized EL spectra of device B1 at voltage from 3 V to 8 V.

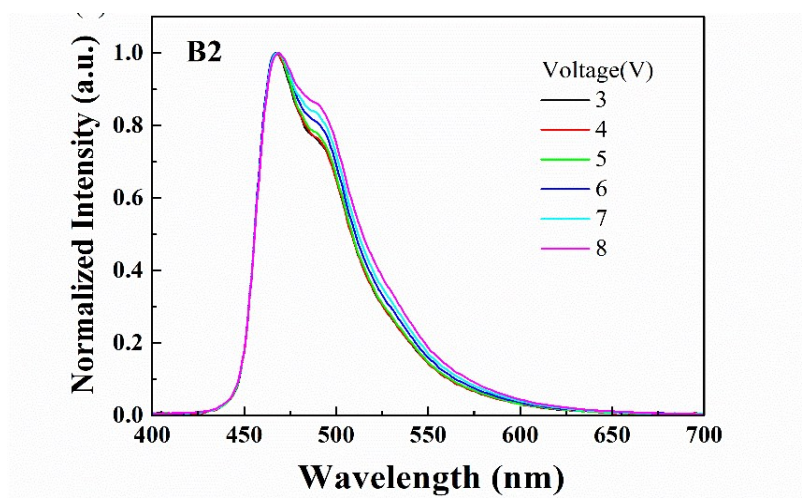


Fig. S4. Normalized EL spectra of device B2 at voltage from 3 V to 8 V.

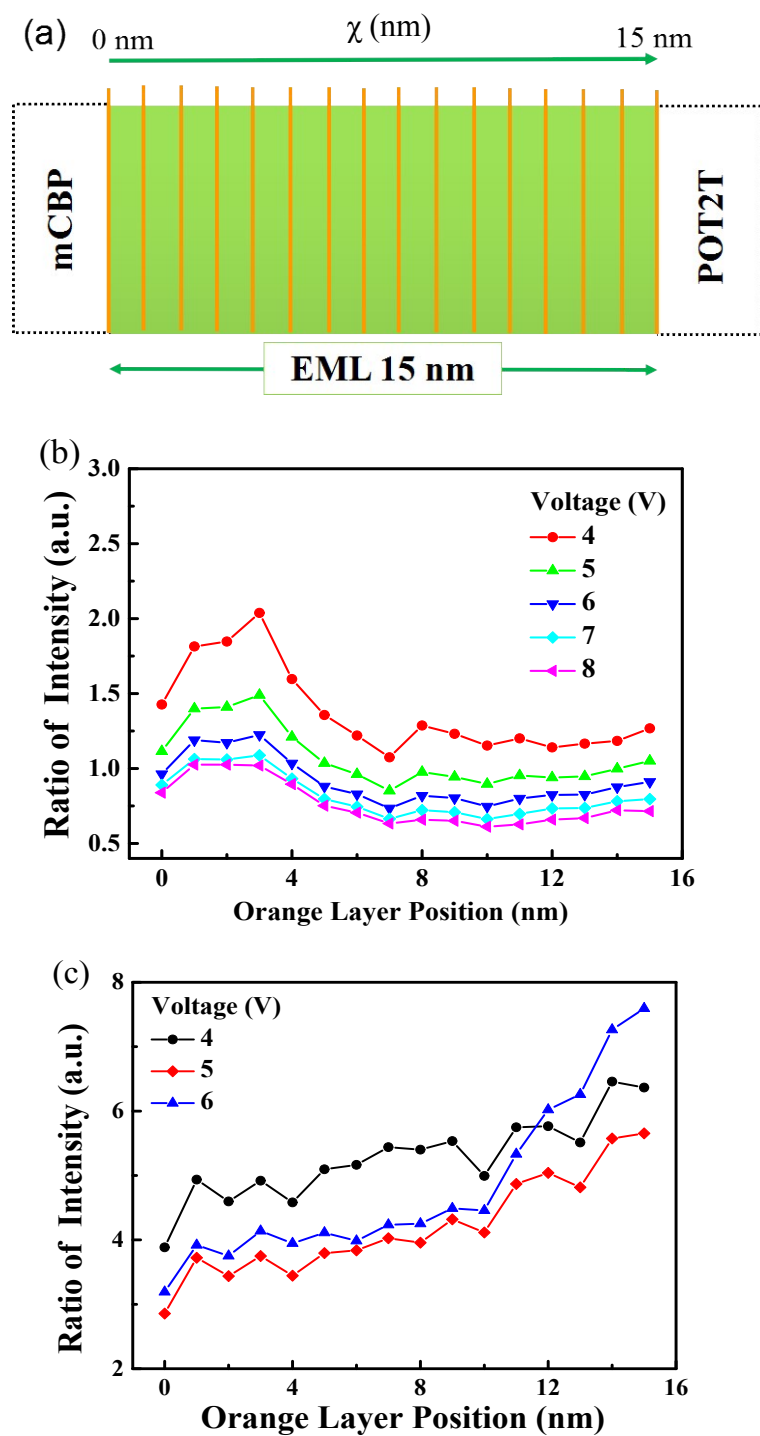


Fig. S5. (a) Schematic diagram for probing local triplet density in EML. An orange phosphorescent ultrathin layer (UTL) is inserted at different positions, where χ is the distance from the interface between mCBP layer and EML. (b) Exciton distribution profile in device B2 at different driving voltages. The ratio of intensity refers to the ratio of orange emission peak intensity to blue intensity as a function of the position of orange thin layer in EML (mCBP:PO-T2T:FIrpic (1:1:10%, 15 nm)).

(c) Exciton distribution profile in device B1 at different driving voltages. The ratio of intensity refers to the ratio of orange emission peak intensity to blue intensity as a function of the position of orange thin layer in EML (mCBP:PO-T2T (1:1, 15 nm)).

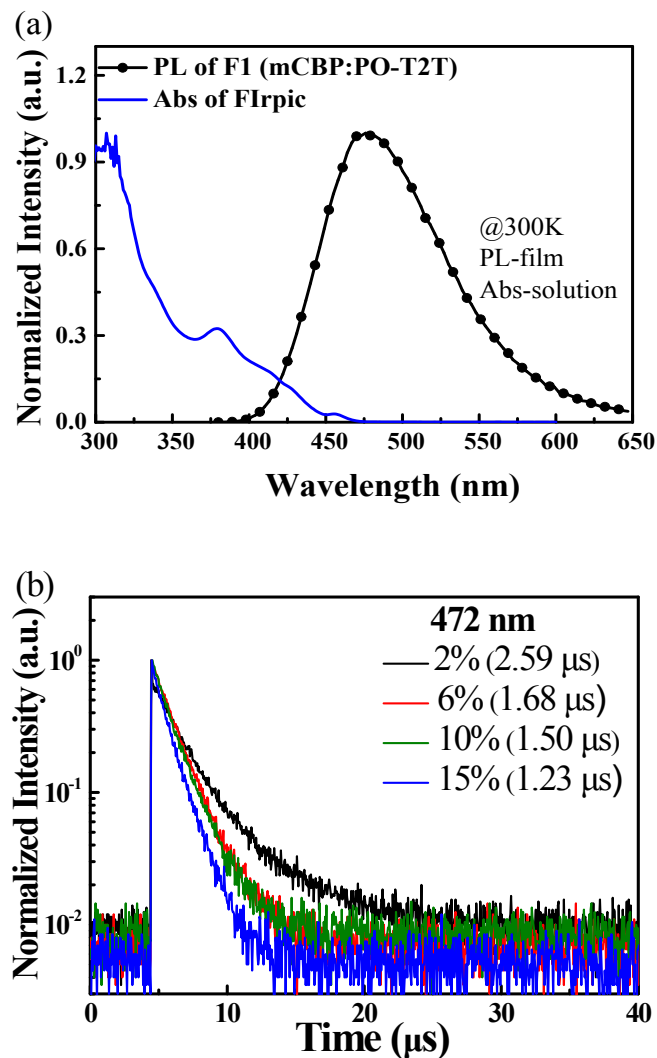


Fig. S6. (a) UV-vis absorption spectra of F1rpic in dichloromethane solution and emission spectra of F1 film. (b) Transient PL decay curves of mCBP:PO-T2T: x% F1rpic films with increasing the F1rpic concentrations from 2 to 15% detected at 472 nm.

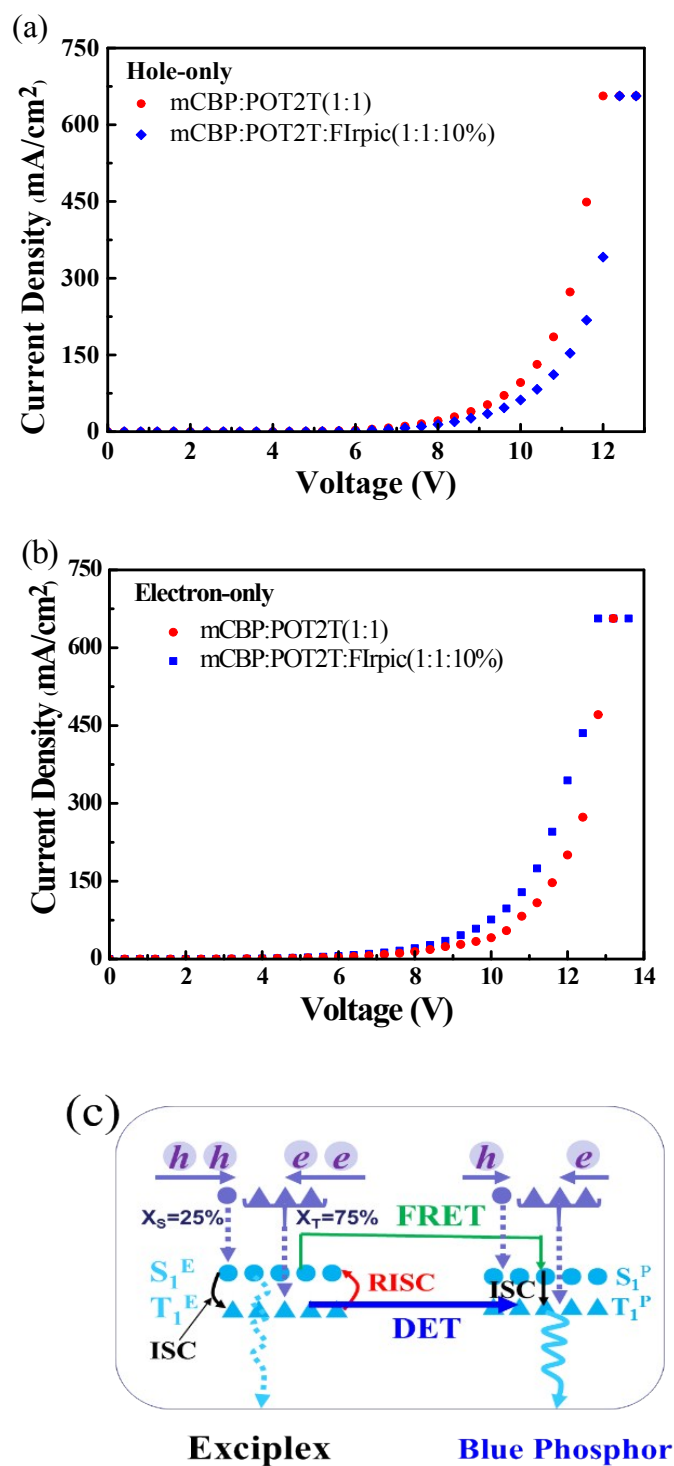


Fig. S7. Current density curves of hole-only (a) and electron-only (b) devices with EML of mCBP:PO-T2T:Flrpic (1:1:10%, 15 nm) or mCBP:PO-T2T (1:1, 15 nm). Hole-only device: ITO / HAT-CN (15 nm) / TAPC (60 nm) / TCTA (5 nm) / mCBP (5 nm) / EML(15 nm) / mCBP (5 nm) / TCTA (5 nm) / TAPC (60 nm) / HAT-CN (15 nm) / Al (150 nm). Electron-only device: ITO / Liq (1.5 nm) / PO-T2T (45 nm) / EML (15 nm) / PO-T2T (45 nm) / Liq (1.5 nm) / Al (150 nm). (c) Proposed emission mechanism of device B2. FRET is the Förster energy transfer process, DET is the

Dexter energy transfer process, ISC denotes the intersystem crossing, RISC indicates the reverse intersystem crossing. According to spin statistics, the proportion of singlet excitons (X_S) is 25% and that of triplet excitons (X_T) is 75% under electrical excitation. S_1^E , T_1^E , S_1^P and T_1^P represent the singlet / triplet level of exciplex and orange phosphorescent emitter, respectively.

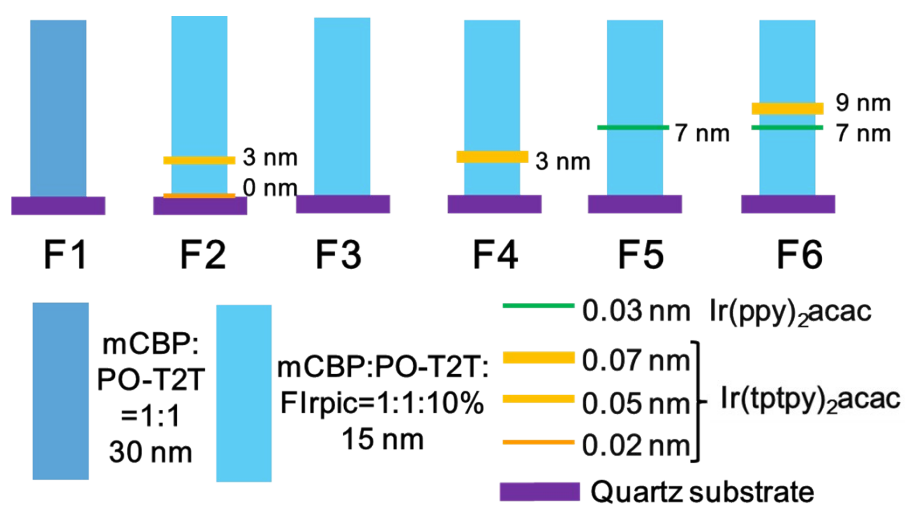


Fig. S8. Schematic diagram of the different films (F1, F2, F3, F4, F5 and F6).

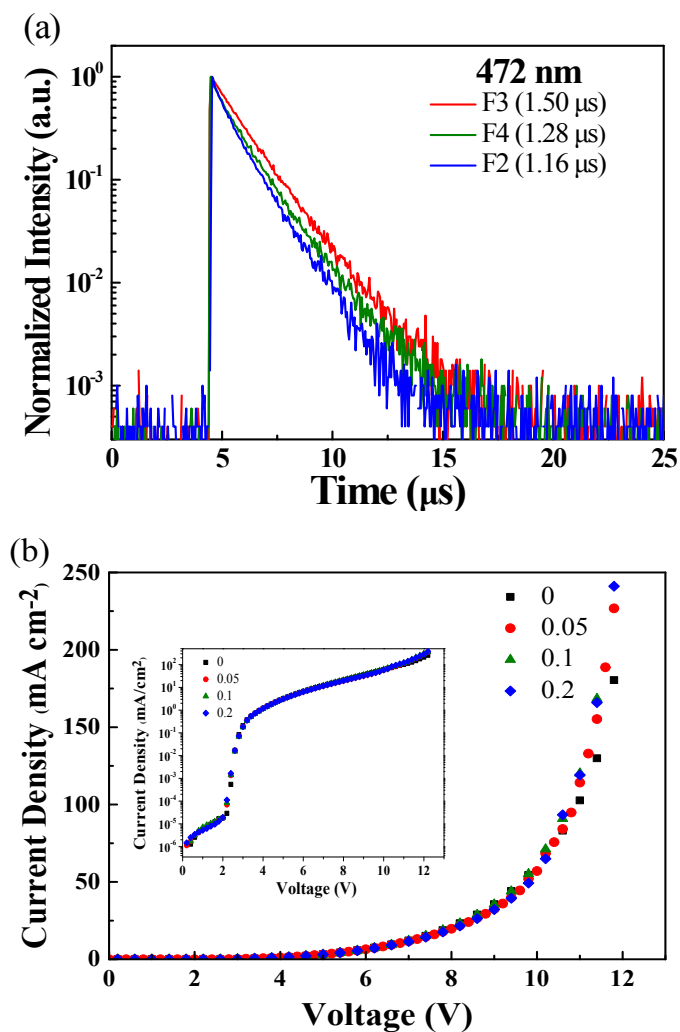


Fig. S9. (a) Transient PL decay curves of F3 and F4 films detected at 472 nm. F3: Quartz / mCBP:PO-T2T:FIrpic (1:1:10%, 15 nm); F4: Quartz / mCBP:PO-T2T:FIrpic (1:1:10%, 3 nm) / Ir(tp_{tpy})₂acac (0.07 nm) / mCBP:PO-T2T:FIrpic (1:1:10%, 12 nm). (b) J–V characteristics of the devices with different thicknesses of orange UTL. The device structure: ITO / HAT-CN (15 nm) / TAPC (60 nm) / TCTA (5 nm) / mCBP(5 nm) / mCBP:PO-T2T:FIrpic (1:1:10%, 7.5 nm) / Ir(tp_{tpy})₂acac (0, 0.05, 0.1, 0.2 nm) / mCBP:PO-T2T:FIrpic (1:1:10%, 7.5 nm) / PO-T2T (45 nm) / Liq (1.5 nm) / Al (150 nm).

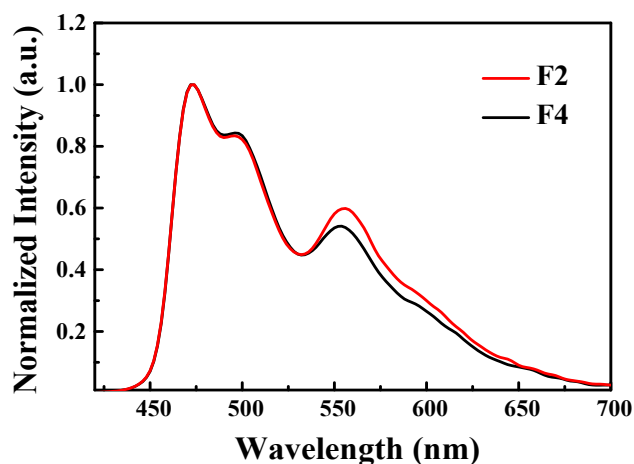


Fig. S10. PL spectra of films (F2 and F4).

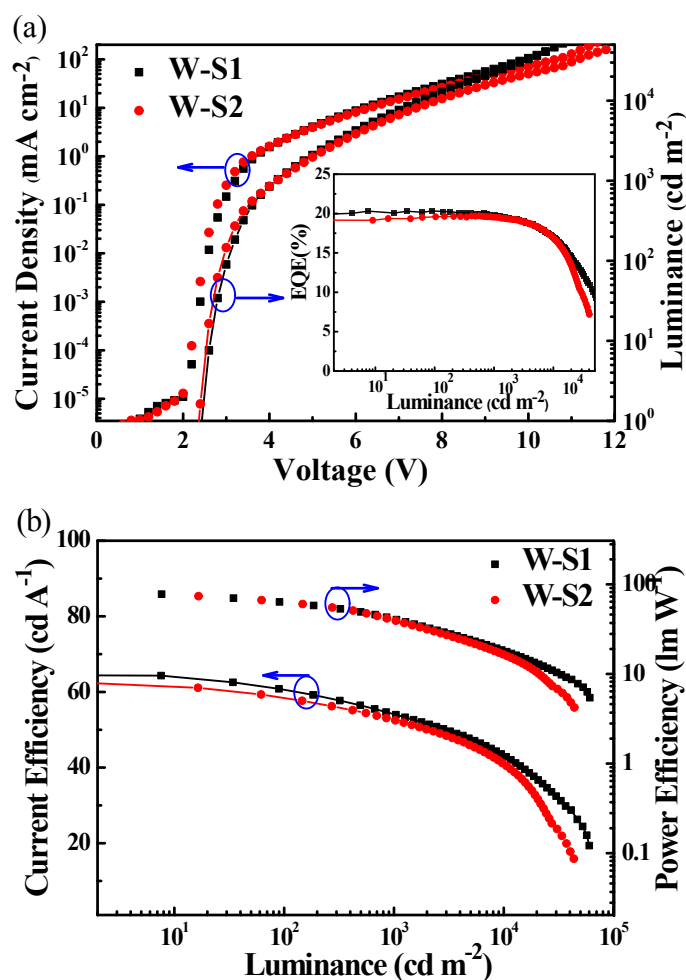


Fig. S11. (a) Current density–luminance–voltage characteristics of the fabricated WOLEDs (W-S1, W-S2). Inset: EQE versus luminance characteristics of the fabricated WOLEDs (W-S1, W-S2). (b) Current efficiency –power efficiency–luminance characteristics of the fabricated WOLEDs (W-S1, W-S2). The structure of W-S1: ITO / HAT-CN (15 nm) / TAPC (60 nm) / TCTA (5 nm) / mCBP (5 nm) / Ir(tptpy)₂acac (0.07 nm) / mCBP:PO-T2T:FIrpic (1:1:10%, 15 nm) / PO-T2T (45 nm) / Liq

(1.5 nm) / Al (150 nm). The structure of W-S2: ITO / HAT-CN (15 nm) / TAPC (60 nm) / TCTA (5 nm) / mCBP (5 nm) / mCBP:PO-T2T:FIrpic (1:1:10%, 9 nm) / Ir(tpptpy)₂acac (0.07 nm) / mCBP:PO-T2T:FIrpic (1:1:10%, 6 nm) / PO-T2T (45 nm) / Liq (1.5 nm) / Al (150 nm).

Table S2 The performance of the representative hybrid WOLEDs

References	^a V _{on} (V)	^b EQE _{max} (%)	^b PE _{max} (lm W ⁻¹)	^d EQE ₁₀₀₀ (%)	^d PE ₁₀₀₀ (lm W ⁻¹)
This work	2.3	22.8	95.3	21.9	55.5
Ref [S1]	2.35	22.45	97.1	16.05	39.8
Ref [S2]	3.06	20.8	51.2	19.6	38.7
Ref [S3]	2.5	25.5	84.1	14.8	24.2
Ref [S4]	2.6	23.8 ^c	62.9 ^c	20.1 ^c	41.7 ^c
Ref [S5]	2.7	15.4	40.2	24.1	11.8
Ref [S6]	-	33.3 ^c	85.3 ^c	22.7 ^c	34 ^c
Ref [S7]	-	-	-	16.1 ^c	37.5 ^c
Ref [S8]	2.4	21 ^c	48.2 ^c	20.2 ^c	26.8 ^c
Ref [S9]	3.2	26	-	16.4	23.3
Ref [S10]	2.62	21.6	59.9	-	43.3
Ref [S11]	2.7	22.3	64.8	-	-
Ref [S12]	2.7	16.4	44	16	37
Ref [S13]	3.3	16.83	40.20	-	-

^a The turn-on voltage measured at 1 cd m⁻² ^b Maximum efficiencies of devices ^c Total efficiencies ^d Measured at 1000 cd m⁻²

References:

- [S1] S. Ying, J. Yao, Y. Chen, D. Ma, *J. Mater. Chem. C*, 2018, DOI: 10.1039/C8TC01736K.
- [S2] D. Zhang, M. Cai, Y. Zhang, D. Zhang, L. Duan, *ACS Appl. Mater. Interfaces*, 2015, **7**, 28693.
- [S3] X. K. Liu, Z. Chen, J. Qing, W. J. Zhang, B. Wu, H. L. Tam, F. Zhu, X. H. Zhang, C. S. Lee, *Adv Mater.*, 2015, **27**, 7079.
- [S4] X. Ouyang, X.-L. Li, L. Ai, D. Mi, Z. Ge, S.-J. Su, *Acs Appl. Mater. Interfaces*, 2015, **7**, 7869.
- [S5] Z. Chen, X.-K. Liu, C.-J. Zheng, J. Ye, X.-Y. Li, F. Li, X.-M. Ou, X.-H. Zhang, *J. Mater. Chem. C*, 2015, **3**, 4283.
- [S6] D. Zhang, L. Duan, Y. Zhang, M. Cai, D. Zhang, Y. Qiu, *Light: Sci. Appl.*, 2015, **4**, e232.
- [S7] G. Schwartz, M. Pfeiffer, S. Reineke, K. Walzer, K. Leo, *Adv. Mater.*, 2007, **19**, 3672.

- [S8] C.-J. Zheng, J. Wang, J. Ye, M.-F. Lo, X.-K. Liu, M.-K. Fung, X.-H. Zhang, C.-S. Lee, *Adv. Mater.*, 2013, **25**, 2205.
- [S9] B. Zhang, G. Tan, C.-S. Lam, B. Yao, C.-L. Ho, L. Liu, Z. Xie, W.-Y. Wong, J. Ding, L. Wang, *Adv. Mater.*, 2012, **24**, 1873.
- [S10] H. Sasabe, J. Takamatsu, T. Motoyama, S. Watanabe, G. Wagenblast, N. Langer, O. Molt, E. Fuchs, C. Lennartz, J. Kido, *Adv. Mater.*, 2010, **22**, 5003.
- [S11] L. Zhu, Y. Zhao, H. Zhang, J. Chen, D. Ma, *J. Appl. Phys.*, 2014, **115**, 244512.
- [S12] Y. Zhao, J. Chen, D. Ma, *ACS Appl. Mater. Interfaces*, 2013, **5**, 965.
- [S13] Y. Miao, K. Wang, B. Zhao, L. Gao, Y. Wang, H. Wang, B. Xu and F. Zhu, *J. Mater. Chem. C*, 2017, **5**, 12474.